Biophysical Chemistry 12 (1980) 143–158


# MAGNETIC CIRCULAR DICHROISM ANALYSIS OF THE IHP EFFECT ON SPIN EQUILIBRIA IN HUMAN FERRIC HEMOGLOBINS [1,2]

Robert E. LINDER, Ruth RECORDS, Günter BART, Edward BUNNENBERG, Carl DJERASSI
*Department of Chemistry, Stanford University, Stanford, CA 94305, USA*

Bo E. HEDLUND, Andreas ROSENBERG
*Department of Laboratory Medicine and Pathology, University of Minnesota, Minneapolis, MN 55455, USA*

Lloyd SEAMANS, Albert MOSCOWITZ
*Department of Chemistry, University of Minnesota, Minneapolis, MN 55455, USA*

Received 20 February 1980

Magnetic circular dichroism (MCD) spectroscopy has been used to explore the connection between optical spectra and the high spin population of several hemoglobins under various conditions. It is found that the effectiveness of IHP in inducing spectral changes can be markedly affected by solvent. For example, the IHP-induced spectral changes in the visible region for nitritomethemoglobin-A in mixed buffer solvent systems (glycerol or polyethylene glycol (PEG), mw 190–210) are more than double those observed in aqueous buffers. We estimate that IHP induces a mix of R/T forms in bis-tris phosphate buffers, for $NO_2^-$metHb that is only about 50% T form. While PEG and glycerol both lead to enhanced IHP-induced spectral differences, they behave differently in two aspects. PEG shifts the visible MCD and absorption spectra of $F^-$metHb-A, supposedly already biased towards the T form by ligand, in the same direction that IHP does. PEG also maximizes the spin state changes with IHP for three R form hemoglobins and $N_3^-$metHb-A, and so appears to stabilize the T form in all cases. Glycerol does not. In addition, the apparent binding constant for $NO_2^-$ to $H_2O$metHb-A differs between these two solvents. Comparison of the data from several hemoglobins leads to the conclusion that the changes in spin state distributions induced by IHP correlate well with quarternary structure for a given hemoglobin. An analogous correlation amongst various proteins between initial spin state distribution (IHP absent) and quarternary structure is not found.

## 1. Introduction

Perutz and his co-workers [1–8] have studied ferric hemoglobins extensively, and have found that IHP[±1] causes changes in their optical spectra that are consistent with the idea that IHP shifts the conformational (R ⇄ T) equilibrium in metHb towards the T form. In more recent work, however, the validity of this interpretation of the spectral changes was questioned [6,7]. We have therefore undertaken a re-examination of this problem using an alternative spectroscopic technique for monitoring optical transitions.

MCD and magneto-optical rotatory dispersion (MORD) have been extensively applied to hemoglobin [9–26] and MCD has found utility in the analysis of spin state distributions in myoglobin [27] and in cytochrome P-450 [28]. However, even though hemoglobin represents a case where spin state information has been

[1] Part LVI in our series on Magnetic Circular Dichroism. For Part LV, see G. Barth, N. Waespe-Sarcevic, R.E. Linder, E. Bunnenberg, C. Djerassi, L. Seamans and A. Moscowitz, J. Chem. Soc. Perkin II (1979) 908.

[2] This work was supported in part by the National Institutes of Health (Grants No. HL-16833 and GM-20276) and the National Science Foundation (Grant No. CHE-7706752).

[±1] Magnetic circular dichroism, MCD; magneto-optical rotatory dispersion, MORD; Inositol hexaphosphate, IHP; polyethylene glycol, PEG; bis-(2-hydroxyethyl)-imino-tris-(hydroxymethyl) methane, bis-tris; high spin/low spin, HS/LS; bis(maleimidomethyl) ether, BME.

linked to a conformational equilibrium [1–8,29,30], an analysis of the spin state populations of hemoglobin on the basis of MCD measurements is not available. This void provides further motivation for our current investigations.

When we began these studies on the MCD of ferric hemoglobin we quickly found that the results were highly dependent upon experimental conditions. Part of the variations could be ascribed to the regeneration of oxyhemoglobin on the separatory column [31], but the rest were found to result from a strong solvent dependence of the effectiveness of IHP in inducing conformational changes. Since such a dependence has not been reported for hemoglobin, we explored these solvent effects in some detail and report here the variation in the spin state distribution of $N_3^-$ metHb-A and $NO_2^-$ metHb-A with IHP and in several buffer/solvent mixtures. We have also studied the $NO_2^-$ metHb derivative of three R form hemoglobins (Wood, Osler, and BME-treated A) and of three hemoglobins (A, S, and F) which undergo the R/T transition. One interesting and unexpected result is that the R and T form populations of $NO_2^-$ metHb-A in phosphate or bis-tris buffers, *in the presence of IHP*, are about equal. In other solvents, IHP causes a much more complete R/T transition.

## 2. Materials and procedures

### 2.1. Sample preparation

Purified oxyhemoglobin-$A_0$ was prepared, as described elsewhere [32], at the University of Minnesota and shipped on ice as ~1 mM tetramer in 0.1N NaCl to Stanford University for spectral analysis. Methemoglobin stock solutions were prepared by oxidizing ~4 ml of oxyhemoglobin stock with potassium ferricyanide (Allied Chem., reagent). Excess reagent was removed by column chromatography (Sephadex G-25 20 cm × 1.8 cm, Pharmacia medium or Dowex 1-X8, 8 cm × 1.8 cm, Polysciences). Some reduction of the methemoglobin to oxyhemoglobin occurs on both columns [31], although appreciably less reduction was observed for the anion exchange column. $HbO_2$ was eliminated with ~5% (molar ratio to heme) potassium ferricyanide. This procedure caused no interference with the IHP-induced spectral differences. The buffers were either phosphate (0.1M, $I \sim 0.2$) or bis-tris (0.05M, 0.1 M NaCl) buffers which were adjusted to obtain pH6.0 or pH7.0 at 5°. IHP (Sigma, phytic acid, sodium salt) 0.1M in distilled water, was titrated to pH7 with HCl. The potassium cyanide (Allied Chem., reagent) solution was titrated only to pH7 with HCl to avoid production of HCN gas and renewed at least monthly. Other stock solutions were 0.1 M in NaCl. Typical concentrations of the reagents in the final Hb solutions were: IHP, 1 mM; $NaN_3$ (MCB, reagent), 1 mM; $NaNO_2$ (Baker reagent) 40 mM; KCN, 1 mM (for heme determination, ~10 mM); glycerol (Eastman spectro grade), 50/50, v/v; PEG (MW190–210, Baker) 50/50, v/v; heme, 0.1 mM. The heme concentrations were determined by conversion to cyanomethemoglobin ($\epsilon^{540}_{mM}$ = 11.0). Unless otherwise noted, spectra were measured at 5.0 ± 0.1 degrees in 1 cm cells.

Trace contaminants in glycerol can drastically alter myoglobin [33]. Our glycerol was found to be satisfactory by the criteria given in [33], and the PEG was tested in a similar fashion on Hb-A. Samples were always prepared on the same day that the measurements were made.

### 2.2. Binding constants

The apparent equilibrium binding constants for $NO_2^-$ ligation of methemoglobin were determined by using the amplitude of the MCD spectrum at 580 nm to monitor the relative concentrations of $NO_2^-$ and $H_2O$metHb during titrations. These binding constants are reported in table 1, and require some comment.

When IHP is present, the Hill plot of the saturation curve (fig. 1) exhibits apparent negative cooperativity (slope < 1 near the midpoint of the curve). The upturn

Table 1
Apparent binding constants for $NO_2^-$metHb binding [a]

| Buffer [b] | no IHP [c] | w/IHP [c] |
|---|---|---|
| phosphate/$H_2O$ | 1500 ± 200 | 800 ± 150 |
| bis-tris/$H_2O$ | 1350 ± 200 | 1000 ± 200 |
| bis-tris/glycerol | 1500 ± 200 | 350 ± 100 |
| bis-tris/PEG | 700 ± 150 | 650 ± 150 |

a) Error bars are the range for triplicate determinations on a single Hb sample.
b) The buffers (pH7.0) were mixed 50/50, v/v with the indicated solvents, 5°.
c) [IHP] ~ 1.0 mM, [heme] ~ 100 μM.

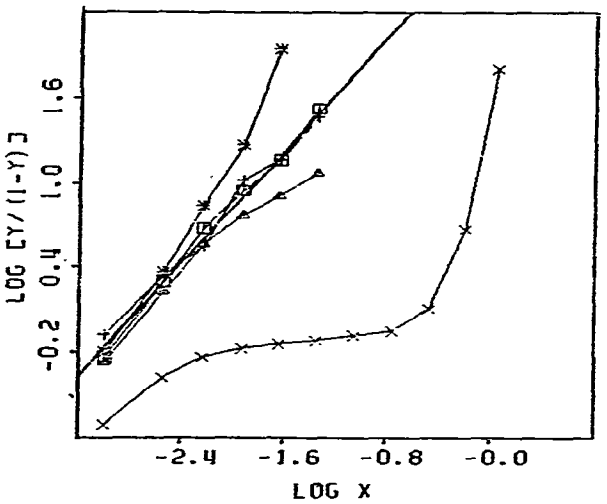


Fig. 1. Hill plots for the binding of $NO_2^-$ to metHb in bis-tris buffer (pH 7.0, 0.5M, 0.1M NaCl, 5°) mixed 50/50 (v/v) with PEG: a) without IHP (+); b) 1.0mM IHP, taking final value as the saturated value (x); c) 1.0 mM IHP, adjusting saturated value to make the region $-3 < \log x < -1$ linear (□); d) taking a saturated value somewhat less than that for c) (△). The solid line is for $n = 1$.

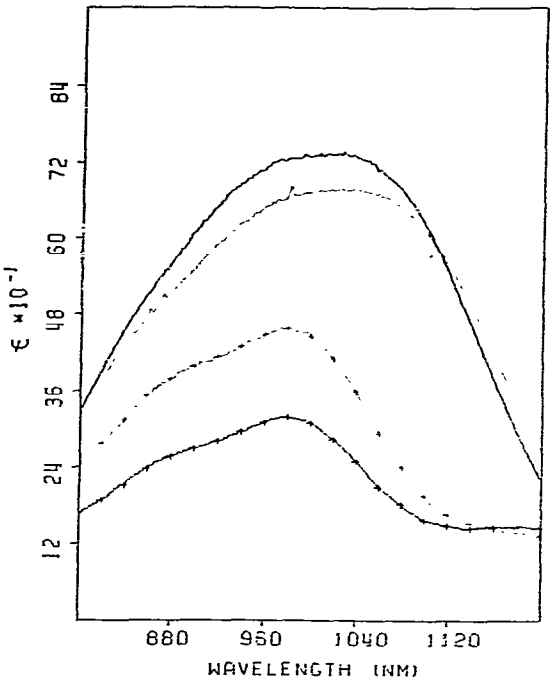


Fig. 2. The near IR absorption spectra of $H_2O$metHb (solid line) and of $NO_2^-$metHb (+), in the presence (lighter lines) and absence (heavier lines) of IHP, in bis-tris buffer (pH 7.0, 0.05M, 0.1M NaCl, 5°).

from hyperbolic behavior occurs at a free ligand concentration, $X$, of about 0.1 M ($\log X \sim -1.0$), which is approximately equal to that of the buffer. Presumably IHP is being displaced by free ligand ($NO_2^-$). Support for this hypothesis is obtained when the titration is continued from the hyperbolic region ($\log X < -1$) with NaCl, which at high concentrations is known to displace IHP: the titration with NaCl produces an upswing in the Hill plot similar to what is observed for $NO_2^-$. Hence we have used free nitrite concentrations of 40 to 50 mM since these concentrations yield 95–98% saturation at 5°, but are below those at which IHP is displaced in a significant amount. The binding constants are determined by first estimating the saturation value in the Hill equation and then successively refining that value until a linear Hill plot is obtained in the region $\log X < -1$. (See fig. 1.)

### 2.3. Verification of the state of ligation

One possible explanation of our data is that IHP displaces half of the iron-bound $NO_2^-$ ions via introduction, by IHP, of strong $\alpha,\beta$ heterogeneity for the $NO_2^-$ binding process. In order to investigate this possibility, we measured the near infrared absorption spectra of aquo- and of nitritomethemoglobin (fig. 2), in the presence and absence of IHP. The observed spectra are consistent only with a shift in the high spin/low spin (HS/LS) equilibrium and not with displacement of $NO_2^-$ from the iron atoms by IHP.

### 2.4. Spectrometry

The spectrometers used were a Cary 14 spectrophotometer and a JASCO J-40 circular dichrometer which is equipped with a 15 kG electromagnet. The normalization equations are

$$\epsilon(\mathrm{M}^{-1}\,\mathrm{cm}^{-1}) = A/l(\mathrm{cm})\,c(\mathrm{M}),$$

$$[\theta]_M(\text{deg cm}^2\text{dmole}^{-1}\text{G}^{-1}) = 100\theta(\text{deg})/H(\text{G})l(\text{cm})c(\text{M}) , \quad (1)$$

where $A$ is the absorbance, $c$ is the total concentration of the hemoglobin (as heme), $l$ is the path length and $H$ is the magnetic field strength (15 kG).

The relatively weak natural circular dichroism (CD) spectrum is measured, stored, and subtracted from the observed MCD + CD curve to give the MCD spectrum. Both absorption and MCD curves are sampled at the rate of one point per nm.

### 2.5. Curve fitting

Two methods of curve fitting were used, mixture analysis by multiple regression and band fitting by nonlinear least squares analysis. The multiple regression model is

$$A/lc = \sum_i (c_i/c)\epsilon_i + \delta_i ,$$

or

$$\theta/Hlc = \sum_i (c_i/c)[\theta]_M^i + \delta_i , \quad (2)$$

where the $\epsilon_i$ or $[\theta]_M^i$ are the normalized spectra of the individual spectral bands as obtained by curve fitting, the $c_i/c$ are the (unknown) relative intensities of each band, and $\delta_i$ is the error term. A discussion of the method and the program used to obtain the least squares best estimate for the $c_i/c$'s is given by Bevington [34].

The nonlinear least squares model for curve fitting the MCD spectra is based upon the assumption of a "rigid shift" with magnetic field by each spectral band [35–37]. Explicit expressions which we use are [37,38]

$$\epsilon = 108.9\nu \sum_i D_i f_i ,$$

$$d\epsilon/d\nu - \epsilon/\nu = 108.9\nu \sum_i D_i f_i' ,$$

or

$$[\theta]_M = -33.53\nu \sum_i A_i f_i' + (B_i + C_i/kT) f_i , \quad (3)$$

where

$$f_i = (g_i)^{-1/b} 2(\Delta\nu_i)^{-1}(\pi)^{-1/2} \times (2^b - 1)^{1/2}\Gamma(1/b)/\Gamma(1/b - 1/2) ,$$

$$f_i' = \delta f_i/\delta\nu = -f_i(g_i)^{-1} 8(\nu - \nu_i)b^{-1}(\Delta\nu_i)^{-2}(2^b - 1) ,$$

$$g_i = 1 + 4(2^b - 1)(\nu - \nu_i)^2/(\Delta\nu_i)^2 ,$$

$$b = a^2 ,$$

and where $A_i$, $B_i$, $C_i$, and $D_i$ are the MCD $A$, $B$, and $C$-values, and the optical dipole strength, respectively, for the $i$th band. The band shape parameters are: $\nu_i$, center frequency; $\Delta\nu_i$, full band width at half maximum; $a$, wing parameter. The wing parameter is zero for gaussian bands and one for lorentzian bands. The intensity parameters ($A_i$, etc.) and the band shape parameters ($\nu_i$, etc.) are varied to minimize the residual sum of squares.

Special precautions are taken to reduce known problems with false minima in this function [39] and include making diverse initial estimates and altering the rate of variation of selected parameters. These actions vary the convergence path so that convergence to the same minimum in each case indicates that the true minimum has been found. Other criteria for judging the validity of curve fitting results include consistency between MCD and absorption results and between curve fitting results and known trends in the data.

The first absorption fits were subject to wide variation, particularly in the halfwidths. It is well known that derivative curves show enhanced spectral resolution over absorption curves and so we investigated the function $d\epsilon/d\nu - \epsilon/\nu$ (eq. (3)) and found that the halfwidths in these fits were much more highly defined. However, the intensities ($D_i$) became less certain. Hence we *simultaneously* fitted $\epsilon$ and $d\epsilon/d\nu - \epsilon/\nu$ to the experimental data. The results were much more satisfactory than those obtained using either function separately. (The experimental derivative function was obtained numerically from the experimental $\epsilon$'s.) The programs used here are our modifications of a program by McKay [40], which uses Marquart's method [39] to estimate the new parameters.

### 2.6. Spin state analysis

Our goal here is to quantitate the effect of perturba-

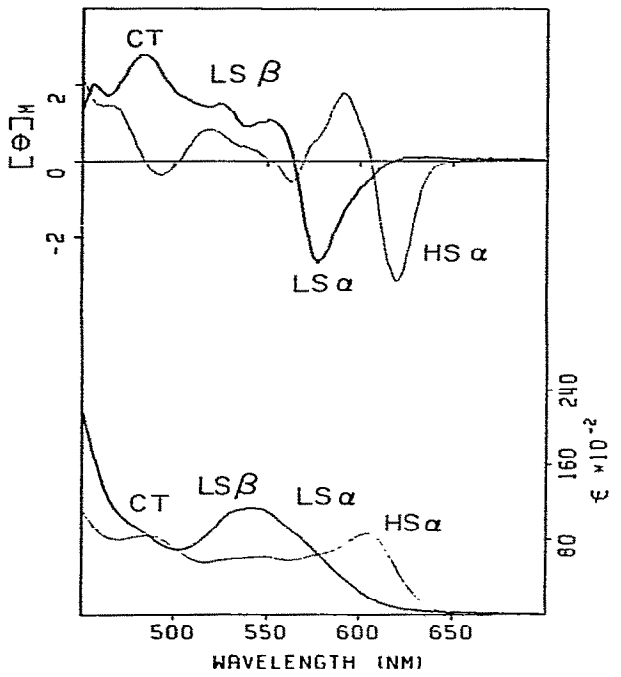


Fig. 3. The visible MCD and absorption spectra of $CN^-$metHb (darker lines) and $F^-$metHb (lighter lines) in phosphate buffer (0.1M, pH 7.0) at 5°.

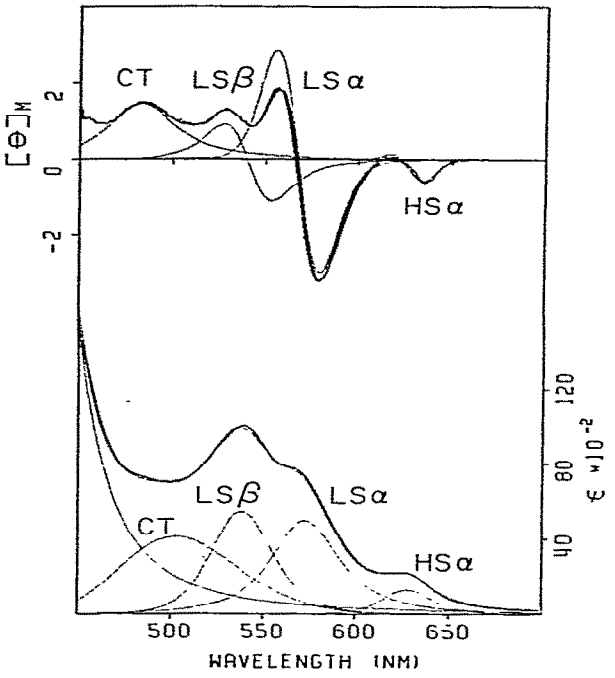


Fig. 4. The visible MCD and absorption spectra of $NO_2^-$metHb (darker lines) in bis-tris buffer (0.05M. 0.1M NaCl, pH 7.0) at 5°. and the deconvolution of these spectra into individual bands (lighter lines). [The sum of the individual bands is also shown.]

tions of the globin on the spin state of the heme iron by analyzing the visible MCD and absorption spectra. We follow Smith and Williams [41]. and require only the spectrum of the mixed spin species and the equilibrium constant. Smith and Williams reasoned that the spectra of eq. (2) are made up of distinct spectral bands.

$$Y_{LS} = \sum_k f_k^{LS}, \quad Y_{HS} = \sum_l f_l^{HS}. \tag{4}$$

where $f_k^{LS}$ or $f_l^{HS}$ are the component bands in the spectra of the pure spin species and the $Y$'s are the total spectra of the pure spin species. The initial unperturbed species is then assumed to be

$$X = \sum_k^{LS} R f_k^{LS} + \sum_l^{HS} (1-R) f_l^{HS} \tag{5}$$

where

$$R = C_{LS}/C = 1 - C_{HS}/C.$$

and where $C_{LS}$, $C_{HS}$, and $C$ are the concentrations of LS, HS, and total heme. The products of $R$ or $(1-R)$ and the $f$'s are found by curve fitting the unperturbed spectrum, $X$, and knowledge of $R$ is sufficient to define the $f_k^{LS}$ and $f_l^{HS}$. The multiple regression model used to fit the perturbed spectar is then

$$X' = \sum_k^{LS} \frac{C_k^{LS}}{C} f_k^{LS} + \sum_l^{HS} \frac{C_l^{HS}}{C} f_l^{HS}. \tag{6}$$

Each regression coefficient is thus an independent estimate of the perturbed spin state populations. Since these estimates are independent, the global estimate of $R'$ is the average of that from either band, i.e.

$$R' = (1 - [HS] + [LS])/2. \tag{7}$$

This procedure tends to minimize concentration errors.

Table 2A
Individual band parameters for nitritomethemoglobin[a)]

| Species | Band | $a$ | $\Gamma$ | $\nu_0$ | $A$ | $B\times10^3$ | $D$ |
|---|---|---|---|---|---|---|---|
| $NO_2^-$metHb | Hs $\alpha$ | 0.685 | 794 | 15906 | – | – | 0.716 |
| | | 0.026 | 483 | 15892 | 0.101 | 0.377 | – |
| | LS $\alpha$ | 0.842 | 1340 | 17431 | – | – | 4.671 |
| | | 0.316 | 912 | 17600 | 3.194 | 0.303 | – |
| | LS $\beta$ | 0.571 | 1361 | 18552 | – | – | 4.236 |
| | | 0.625 | 1222 | 18474 | 2.142 | 0.767 | – |
| | CT[b)] | 0.010 | 2956 | 19804 | – | – | 5.964 |
| | | 0.809 | 1866 | 20603 | 0.414 | –5.116 | – |
| | Soret | 0.803 | 1903 | 24390 | – | – | 131.5 |

Table 2B
Individual band parameters for azidomethemoglobin

| Species | Band | $a$ | $\Gamma$ | $\nu_0$ | $A$ | $B\times10^3$ | $D$ |
|---|---|---|---|---|---|---|---|
| $N_3^-$metHb | HS $\alpha$ | 0.124 | 1370 | 15740 | – | – | 0.763 |
| | | 0.203 | 318 | 15777 | 0.0059 | 0.075 | – |
| | LS $\alpha$ | 0.467 | 947 | 17313 | – | – | 2.997 |
| | | 0.433 | 763 | 17361 | 2.657 | 2.84 | – |
| | LS $\beta$ | 0.520 | 1194 | 18441 | – | – | 4.575 |
| | | 0.691 | 1015 | 18560 | 1.058 | –2.16 | – |
| | CT[b)] | 0.012 | 4178 | 19398 | – | – | 9.686 |
| | | 0.654 | 2582 | 20920 | –0.504 | –7.40 | – |
| | Soret | 0.810 | 2496 | 23964 | – | – | 65.67 |

Table 2C
Individual band parameters for hydroxymethemoglobin

| Species | Band | $a$ | $\Gamma$ | $\nu_0$ | $A$ | $B\times10^3$ | $D$ |
|---|---|---|---|---|---|---|---|
| $OH^-$metHb | HS $\alpha$ | 0.086 | 882 | 16596 | – | – | 2.385 |
| | | 0.003 | 791 | 16663 | 1.224 | –1.36 | – |
| | LS $\alpha$ | 0.032 | 899 | 17314 | – | – | 2.984 |
| | | 0.741 | 737 | 17328 | 3.461 | 1.95 | – |
| | LS $\beta$ | 0.070 | 1371 | 18449 | – | – | 6.849 |
| | | 0.801 | 1122 | 18560 | 2.911 | –1.66 | – |
| CT | CT | 0.014 | 2060 | 20181 | – | – | 2.590 |
| | Soret | 0.823 | 2299 | 24390 | – | – | 149.4 |

a) The parameters in table 2 (see eq. (3) for definition) reproduce the fitted specta and are not normalized for the spin state populations, i.e. the intensities ($I$) in tables 2A–D are $R \cdot I$ or $(1-R) \cdot I$, depending upon the spin state associated with the band. To get the intensity associated with the pure spin state for a given band, divide the table entry by $R$ or $1-R$.
b) The CT bands are obviously not of the same origin in MCD and absorption. See text.

### 2.7. Calibration–internal and external

If the $R$'s for each species can be obtained by independent methods, such as magnetic susceptibility measurements, we can use these values to scale the separated bands in eq. (5) and thereby calibrate the procedure. If $R$ is not known, we may determine it, and its changed value $R'$ in the perturbed case, from the multiple regression results *if* we assume that the differences between the spectra of the perturbed and unperturbed protein are due solely to changes in the spin state populations. In this case, eq. (6) becomes

Table 2D
Individual band parameters for aquomethemoglobin

| Species | Band | $a$ | $\Gamma$ | $\nu_0$ | $A$ | $B\times10^3$ | $D$ |
|---|---|---|---|---|---|---|---|
| $H_2$OmetHb | HS $\alpha$ | 0.121 | 808 | 15822 | – | – | 1.473 |
| | | 0.084 | 526 | 15834 | 0.471 | 0.551 | – c) |
| | | 0.010 | 357 | 16101 | 0.044 | 0.632 | – c) |
| | LS $\alpha$ | 0.023 | 2166 | 17098 | – | – | 2.919 |
| | | 0.037 | 868 | 17027 | 0.370 | 0.830 | – |
| | LS $\beta$ | 0.023 | 722 | 18519 | – | – | 0.329 |
| | | 0.058 | 575 | 18557 | 0.222 | 0.356 | – |
| | CT | 0.014 | 2383 | 19786 | – | – | 8.223 |
| | Soret | 0.832 | 2088 | 25000 | – | – | 133.6 |

c) These two bands are summed to give the HS $\alpha$ band.

$$X' = \sum_k^{LS} \frac{R'}{R} R f_k^{LS} + \sum_l^{HS} \frac{1-R'}{1-R}(1-R) f_l^{HS}. \quad (8)$$

Thus multiple regression with the band as fitted on the unperturbed spectrum, $R$ or $1-R$ times the $f$'s (the unnormalized basis set), yields the regression coefficients $R'/R$ and $(1-R')/(1-R)$ for the appropriate bands. This yields two equations and two unknowns and so we may solve for $R$ and $R'$.

## 3. Spectroscopic results and discussion

### 3.1. Spectra of high and low spin forms of methemoglobin

The low spin methemoglobins are typified by cyanomethemoglobin which is low spin at accessible temperatures [42,43]. Likewise, fluoromethemoglobin is typical of the high spin forms [5]. The visible MCD and absorption spectra of $CN^-$metHb (100% low spin [42]) and of $F^-$metHb (100% high spin [5]) are given in fig. 3. The primary difference between the MCD of these two species lies in the position of the $\alpha$ band (crossover ~560 nm in $CN^-$metHb: ~605 nm in $F^-$metHb). The maximum absorption of $CN^-$metHb is at ~540 nm (due to two bands, the LS $\alpha$ and the LS $\beta$ bands) [‡2].

[‡2] The nomenclature is LS = low spin, HS = high spin, $\alpha = Q_{0-0}\pi\rightarrow\pi^*$, $\beta = Q_{0-1}\pi\rightarrow\pi^*$, CT = mixed $\pi\rightarrow\pi^*$ and charge transfer excitations. See Smith and Williams [36,37] for spectroscopic background and band assignments. In particular, they show that the HS $\alpha$ band has some charge transfer character and explore ligand variations.

while $F^-$metHb shows two predominant absorption maxima (~605 nm, the HS $\alpha$ band, and ~490 nm, the CT band).

### 3.2. Deconvolution of methemoglobin spectra

Nonlinear least squares fitting was used to obtain the band structure of $NO_2^-$metHb, $N_3^-$metHb, $OH^-$metHb and $H_2$OmetHb. Generally, the spectra were fitted with the HS $\alpha$, LS $\alpha$, LS $\beta$, and CT band and, in the case of the absorption spectra, the tail of the Soret band. An example of the comparison of fitted and experimental spectra and the components of the fitted spectra is given in fig. 4 ($NO_2^-$metHb) The spectral parameters of the components for $NO_2^-$, $N_3^-$, $OH^-$, and $H_2$OmetHb are tabulated in tables 2A–2D.

Two situations require elaboration. First, the CT band is of mixed origin as can be seen by comparing center frequencies in tables 2A and 2B for the CT band. Evidently two bands exist in this region, one strong in absorption but not in MCD, and vice versa. The connection between spin state and band intensity is not unique in the CT region and we will largely ignore these bands. Second, the very weak HS $\alpha$ band in the azidomethemoglobin MCD spectrum was fitted first and subtracted from the experimental spectrum. The resultant curve was then used to obtain the remaining bands. If this procedure was not followed, overlap from the LS $\alpha$ band rendered the fitted parameters for the HS $\alpha$ band unreliable. Because of the mixed nature of the CT band and because the LS$\beta$ band is weak in MCD, we choose the HS $\alpha$ and LS $\alpha$ bands as the analytical bands for spin state analysis.

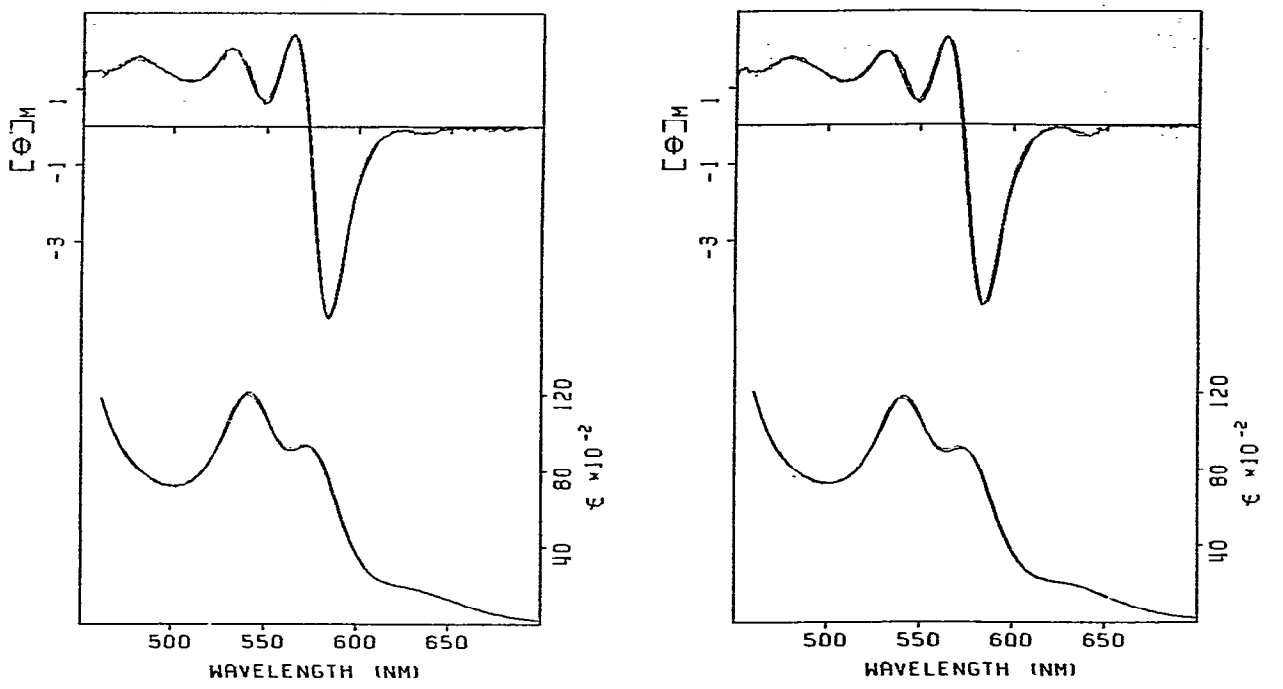


Fig. 5. A) Experimental MCD and absorption spectra (darker lines) and multiple regression fits (lighter lines) for $N_3^-$metHb in bis-tris buffer (pH 7.0, 0.05M, 0.1 M NaCl, 5°) in the absence of IHP, [heme] ~ 100μM. B) Same as A, but in the presence of 1.0 mM IHP.

### 3.3. Spin state analysis

The data were analyzed using eq. (8) as the multiple regression model and the fitted bands in table 2 as the basis set. An example of the resulting calculated spectra along with the experimental spectra is given in fig. 5. Here the calculated spectra mimic the experimental spectra quite well. In particular, the red shift in the HS α band in MCD does not appear to have affected the reconstruction.

Eq. (8) for $N_3^-$metHb is calibrated with the magnetic susceptibility data obtained by Iizuka and Kotani [42]; these data yield a value for $R$ of 0.916 for $N_3^-$metHb at 5°. With this value for $R$, the appropriate relative band intensities are converted to spin state percentages which are presented in table 3.

We see that the spin state populations determined by MCD and absorption agree very nicely when IHP is absent, and, with one exception, the changes in the low spin content which occur upon addition of IHP agree well. However, the changes in high spin content with IHP are underestimated badly from absorption data. Examination of the fits reveals no obvious reason for this and we conclude that an absorption band from the LS form is present in the HS α region. Such a band has been noted in azidometmyoglobin by Eaton and Hochstrasser [44] who find a broad $z$-polarized band at 650 nm and associate this band with the low spin form. $Z$-polarized bands are expected to be much weaker in MCD than are the $x$, $y$-polarized degenerate excitations since the latter transitions exhibit strong A terms. We measured the MCD spectrum of $N_3^-$metHb at ~−20° (where $R > 0.96$) and indeed find that the HS α MCD band is essentially gone. In MCD, therefore, the intensity of the HS α band is a valid measure of the high spin fraction in $N_3^-$metHb. whereas this is not the case in absorption.

Table 3
Spin state populations in mixed solvents – azidomethemoglobin

| Buffer | IHP(mM) | %HS | %LS | Σ(%) | ΔHS(%) | ΔLS(%) |
|---|---|---|---|---|---|---|
| MCD method [b),c)] | | | | | | |
| phosphate/$H_2O$ | 0 | 8.6±0.4 | 93.4±0.9 | 102.0 | +5.5±1.3 | –2.4±1.8 |
| | 1 | 14.1±1.2 | 91.0±1.6 | 105.1 | | |
| bis/tris/$H_2O$ | 0 | 8.4±0.8 | 95.2±0.2 | 103.6 | +5.3±0.8 | –3.9±0.4 |
| | 1 | 13.7±0.1 | 91.3±0.3 | 105.0 | | |
| bis-tris/glycerol | 0 | 8.2±1.1 | 90.4±0.4 | 98.6 | +5.1±1.3 | –5.3±0.7 |
| | 1 | 13.2±0.7 | 85.1±0.6 | 98.3 | | |
| bis-tris/PEG | 0 | 11.1±0.4 | 89.9±1.7 | 101.0 | +8.1±0.9 | –7.0±1.8 |
| | 1 | 20.9±0.8 | 83.0±0.5 | 103.9 | | |
| Absorption method [c),d)] | | | | | | |
| phosphate/$H_2O$ | 0 | 9.1±0.1 | 91.6±0.9 | 100.7 | +1.4±0.1 | –4.6±1.1 |
| | 1 | 10.5±0.1 | 87.0±0.7 | 97.5 | | |
| bis-tris/$H_2O$ | 0 | 9.2±0.1 | 90.0±0.1 | 99.2 | +1.1±0.1 | –4.2±0.3 |
| | 1 | 10.3±0.1 | 85.8±0.1 | 96.1 | | |
| bis-tris/glycerol | 0 | 10.1±0.3 | 88.9±2.1 | 99.0 | +0.3±0.4 | –5.1±2.3 |
| | 1 | 10.4±0.3 | 83.8±1.0 | 94.2 | | |
| bis-tris/PEG | 0 | 9.8±0.2 | 93.7±0.7 | 103.8 | +2.9±0.2 | –7.6±1.1 |
| | 1 | 12.7±0.1 | 86.1±0.8 | 98.8 | | |

a) Buffers (pH 7.0) are mixed 50/50, v/v, with the indicated solvents; 5°.
b) Using the HS α and LS α bands, $R = 0.916$.
c) Error bars are ±1σ.
d) Using the HS α and LS β bands, $R = 0.916$.

### 3.4. $NO_2^-$ metHb

Using eq. (8) as the multiple regression model and the fitted bands of fig. 4 as the basis set, we have analyzed the absorption and MCD spectra of $NO_2^-$ metHb for different perturbations. The experimental and calculated spectra for $NO_2^-$ metHb in bis-tris buffer at pH 7.0 with and without IHP are shown in fig. 6. Comparison of the calculated and experimental spectra shows that the changes with IHP are reasonably well represented even though these changes are quite large.

$NO_2^-$ metHb is not completely characterized and reliable magnetic susceptibility data is not available. Hence we used the internal calibration procedure given earlier to estimate the low spin fraction and obtained $R = 0.70$ (5°). Using this value for $R$ and the relative band intensities, we obtained the spin state populations of table 4. In view of the magnitudes of the changes in populations, the agreement between MCD and absorption on the one hand and between ΔHS and ΔLS on the other is quite good. The change in spin state populations with IHP ranges from 13% to over 30%.

### 3.5. Comparison of calibration procedures

At the end of section 2, we presented two ways to apply the multiple regression equations, one based upon prior know ledge of the spin state equilibrium under reference conditions and the other based upon the assumption that IHP alters only the spin state equilibrium constant. A comparison of the results of spin state analysis by both methods is made in table 5, and the comparison shows a very satisfactory check between the two procedures when MCD data are used. The % increases in high spin state with IHP (ΔSS) agree to within 1% with one exception. This exception ($\delta\Delta SS \approx 2.3\%$ for $NO_2^-$ metHb in bis-tris/PEG) is an extreme case ($\Delta SS > 30\%$), so that on a relative basis the agreement is still satisfactory We conclude that either procedure is basically sound for MCD data. If one uses absorption data the analysis of the $NO_2^-$ metHb data is

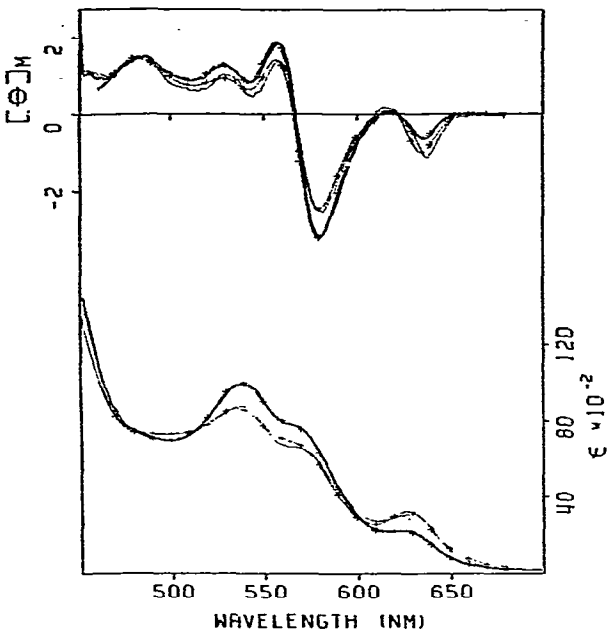


Fig. 6. Experimental MCD and absorption spectra (solid lines) and multiple regression fits (+) for $NO_2^-$metHb in bis-tris buffer (pH 7.0, 0.05 M, 0.1 M NaCl, 5°) in the presence (lighter lines) and absence (darker lines) of 1.0 mM IHP, [heme] ~ 100 μM.

satisfactory, but that for $N_3^-$metHb reflects serious errors due to problems in isolating the HS α absorption band. These errors are reflected primarily in the values of $R$ calculated from eq. (8).

### 3.6. Stability of analysis under band shifts

We have investigated the effect of the HS α band red shift with IHP on the analysis. We expanded the band shape function in a Taylor's series in $\delta\nu$, included these functions in the fit. and evaluated the calculated spin state populations. The results are summarized in table 6A as the variance between three cases: 1) no shift, 2) HS α shift, 3) HS α and LS α shift. It is obvious from the table that the MCD procedure is much more stable towards band shifts than is the one using absorption data. This occurs because the MCD bands overlap each other much less than do the absorption bands.

We also calculated the % LS of $NO_2^-$metHb-A in bis-tris/PEG versus the band shift of the MCD HS α band. These results are given in table 6B and show that the % LS is overestimated somewhat (2.1%) by current procedure. Since this value is small when compared to the % change with IHP (~30%). we can neglect this error for now, but note the result for future improvement of the method.

Table 4
Spin state populations in mixed solvents – nitritomethemoglobin

| Method | Buffer[a] | IHP (mM) | %HS | %LS | Σ (%) | ΔHS (%) | ΔLS (%) |
|---|---|---|---|---|---|---|---|
| MCD[b] | phosphate/$H_2O$ | 0 | 35.9±0.5 | 67.8±0.5 | 103.7 | | |
| | | 1 | 49.3±0.4 | 54.1±1.1 | 103.4 | +13.4±0.6 | −13.7±1.2 |
| | bis-tris/$H_2O$ | 0 | 30.2±1.0 | 70.0±0.5 | 100.2 | | |
| | | 1 | 48.4±0.9 | 52.6±0.5 | 101.0 | +18.2±1.3 | −17.4±0.7 |
| | bis-tris/glycerol | 0 | 30.8±1.5 | 71.6±0.5 | 102.4 | | |
| | | 1 | 56.2±0.2 | 43.1±0.3 | 99.3 | +25.4±1.5 | −28.5±0.6 |
| | bis-tris/PEG | 0 | 34.2±0.8 | 60.9±1.2 | 95.1 | | |
| | | 1 | 61.4±0.4 | 26.8±0.1 | 88.2 | +27.2±0.9 | −34.1±1.2 |
| Abs[c] | phosphate/$H_2O$ | 0 | 38.2±0.2 | 65.5±0.2 | 103.7 | | |
| | | 1 | 53.7±0.2 | 50.7±0.7 | 104.4 | +15.5±0.3 | −14.8±0.7 |
| | bis-tris/$H_2O$ | 0 | 30.9±0.3 | 70.6±0.5 | 101.5 | | |
| | | 1 | 52.6±0.2 | 50.3±0.2 | 102.9 | +21.7±0.4 | −20.3±0.5 |
| | bis-tris/glycerol | 0 | 30.4±0.4 | 70.5±0.7 | 100.9 | | |
| | | 1 | 65.9±0.2 | 42.2±0.3 | 108.1 | +35.5±0.4 | −28.3±0.8 |
| | bis-tris/PEG | 0 | 38.0±1.4 | 58.3±0.6 | 96.3 | | |
| | | 1 | 73.7±1.7 | 24.7±0.4 | 98.4 | +35.7±2.2 | −33.6±0.7 |

[a] Buffers (pH7.0) are mixed 50/50, v/v, with the indicated solvents; 5°.
[b] Using the HSα and LSα bands, $R = 0.7$. [c] Using the HSα and LSβ bands, $R = 0.7$.

Table 5
Comparison of calibration procedures [a]

| Species | Buffer [b] | External calibration [c] | | Internal calibration [d] | |
|---|---|---|---|---|---|
| | | SS | ΔSS | SS | ΔSS |
| $NO_2^-$metHb | phosphate/$H_2O$ | 66.0 (63.6) | −13.6 (−15.2) | 64.9 (64.2) | −13.1 (−14.5) |
| | bis-tris/$H_2O$ | 66.9 (69.5) | −17.8 (−21.0) | 70.8 (71.0) | −17.6 (−20.4) |
| | bis-tris/glycerol | 70.4 (70.0) | −27.0 (−31.9) | 67.4 (74.4) | −26.8 (−29.9) |
| | bis-tris/PEG | 63.4 (60.2) | −30.6 (−34.6) | 58.7 (62.0) | −32.9 (−35.7) |
| $N_3^-$metHb | phosphate/$H_2O$ | 92.3 (91.2) | −2.8 (−3.0) | 96.4 (75.0) | −1.7 (−3.8) |
| | bis-tris/$H_2O$ | 93.4 (90.4) | −4.6 (−2.7) | 93.6 (71 4) | −3.9 (−3.4) |
| | bis-tris/glycerol | 91.2 (89.4) | −5.2 (−2.7) | 91.5 (34.1) | −5.4 (−2.0) |
| | bis-tris/PEG | 89.5 (90.6) | −7.6 (−6.4) | 92.0 (71.4) | −7.2 (−8.5) |

[a] Results from absorption data are given in parentheses.
[b] Buffers (pH 7.0) are mixed 50/50, v/v, with the indicated solvent, 5°.
[c] Calibration is either from magnetic susceptibility ($N_3^-$metHb) or from averaging internal calibration results from earlier spectra ($NO_2^-$metHb). In either case, only one $R$-value is used for all data.
[d] Each set of data is internally calibrated using eq. (8).

Table 6A
Variance due to λ shifts [c]

| Buffer [a] | ΔSS (MCD) | ΔSS (Abs) |
|---|---|---|
| phosphate/$H_2O$ | 14.4±0.4 | 14.9±3.0 |
| bis-tris/$H_2O$ | 17.0±0.2 | 20.8±2.8 |
| bis-tris/PEG | 30.3±0.2 | 34.3±4.9 |

Table 6B
Change in calculated % LS for nitritomethemoglobin-A in bis-tris/PEG solvent with red shifts of the HS α library band.

| %LS | δλ (nm) |
|---|---|
| 26.8 | 0 |
| 26.1 | 0.5 |
| 25.7 | 1.0 |
| 25.3 | 1.5 |
| 25.1 | 2.0 |
| 24.9 | 2.5 |
| 24.7 | 3.0 |
| 24.7 | 3.5 |
| 24.7 | 4.0 |

[a] The indicated buffer (pH 7.0, 5°) is mixed 50/50, v/v, with the indicated solvent.
[b] The derivatives (with respect to frequency) of the HS α and LS α bands are added as indicated to the multiple regression basis set.
[c] The standard deviation is that among the three estimates of ΔSS; calculated with the original basis, adding the HS α band shift, and adding the HS α and LS α band shifts.

### 3.7. Errors

We have indicated only replication errors in all tables, usually as the variance among three solutions all made at the same time from the same reagents and measured on the same day. This procedure was follow-

Table 7
Sample preparation and handling error.

A. ΔSS for $NO_2^-$metHB in bis-tris buffer, pH7, 5°.

| ΔSS [a] |
|---|
| 19.0 |
| 17.4 |
| 17.8 |
| 18.0 |
| 17.9 |
| 15.7 |
| 17.0 |
| 17.5±1.0 |

B. ΔSS for $NO_2^-$metHb in mixed solvents.

| buffer/solvent | ΔSS (preparation 1) | ΔSS (preparation 2) |
|---|---|---|
| bis-tris/glycerol | 27.0±0.8 | 33.8±1.1 |
| bis-tris/PEG | 30.7±0.7 | 36.2±1.1 |

[a] ΔSS = SS (no IHP) − SS (w/IHP).

Table 8
A. IHP Effect – pH differences [a], ionic strength differences [b]

| Buffer | ΔSS (MCD) [c] | ΔSS (Abs) [c] |
|---|---|---|
| bis-tris, pH 6 [a] | 16.6±0.9 | 18.0±0.4 |
| bis-tris, pH 7 [a] | 19.0±1.0 | 19.8±0.5 |
| bis-tris, pH 7 [b] | 17.8±0.8 | |

B. IHP effect–concentration dependence [a]

| Concentration | ΔSS |
|---|---|
| $\sim 10^{-4}$ M | 17.5±1.0 [d] |
| $\sim 10^{-3}$ M | 17.8 [e] |

a) $NO_2^-$metHb, buffers (0.05 M, 0.1 M NaCl, 5°).
b) Same as in a) but diluted 50/50 with $H_2O$.
c) ΔSS in the percentage increase in the high spin population upon addition of IHP. Error bars are ±1σ, triplicate determinations.
d) Based on seven determinations.
e) Single determination.

ed to minimize variance from sample preparation and to allow direct comparison between results. The variations which are due to the initial Hb preparation (purification, storage, or shipping) or which occur during sample makeup (reagent variations, column conditions) may exceed the analytical error. Two sets of data bear on this point: 1) a set of seven determinations of ΔSS for $NO_2^-$metHb in bis-tris buffer (pH 7) obtained over a year's time and from several Hb preparations (table 7A), and 2) a pair of spin state analyses for $NO_2^-$ metHb in the mixed buffer/solvent systems (table 7B). From table 7A, we see that the inherent reproducibility is about 1% in ΔSS, even with preparative errors included, in the absence of PEG or glycerol. When PEG or glycerol is present (table 7B), the variations are greater, for reasons not yet understood. However, either set of values in table 7B is consistent with our arguments.

Other errors include those caused by the presence of additional species, as for example the presence of $OH^-$metHb in $H_2O$metHb solutions. Problems arise in this instance because of the large degree of overlap between the spectra of $OH^-$- and $H_2O$metHb. Further, these problems are exacerbated by band shifts upon the addition of IHP and hence a spin state analysis by the method outlined above is not feasible in this special case.

## 4. Spin state results and discussion

### *4.1. IHP effect – pH, ionic strength heme concentration dependence*

In the initial stages of this work, several variables could possibly have caused the spectral variations which were later ascribed to small amounts of $HbO_2$ and to solvation effects. Hence we examined variations in pH, ionic strength, and heme concentration. The results are given in table 8. Except for a very small possible effect due to pH, these variables cause no change in the ΔSS values in the ranges studied.

Table 9
IHP effect – solvent dependence.

| Ligand | Buffer/Solvent [a] | SS (no IHP) [b],[c] | SS (w/IHP) [b],[c] | ΔSS [c],[d] |
|---|---|---|---|---|
| $N_3^-$ | phosphate/$H_2O$ | 92.4±0.5 | 88.4±1.0 | 4.0±1.1 |
| | bis-tris/$H_2O$ | 93.4±0.4 | 88.8±0.2 | 4.6±0.4 |
| | bis-tris/glycerol | 91.1±0.6 | 86.0±0.5 | 5.1±0.8 |
| | bis-tris/PEG | 89.4±0.9 | 81.0±0.5 | 8.4±1.0 |
| $NO_2^-$ | phosphate/$H_2O$ | 66.0±0.4 | 52.4±1.1 | 13.6±1.2 |
| | bis-tris/$H_2O$ | 69.9±0.6 | 52.1±0.5 | 17.8±0.8 |
| | bis-tris/glycerol | 70.4±0.8 | 43.5±0.2 | 26.9±0.8 |
| | bis-tris/PEG | 63.4±0.7 | 32.8±0.2 | 30.6±0.7 |

a) The buffer (ph 7.0) is diluted with the indicated solvent 50/50, v/v; 5°.
b) SS is the % low spin population from MCD measurements.
c) Error bars are ±1σ.
d) ΔSS is the percentage increase in the high spin population upon addition of IHP. (ΔSS = SS (no IHP) – SS (w/IHP)).

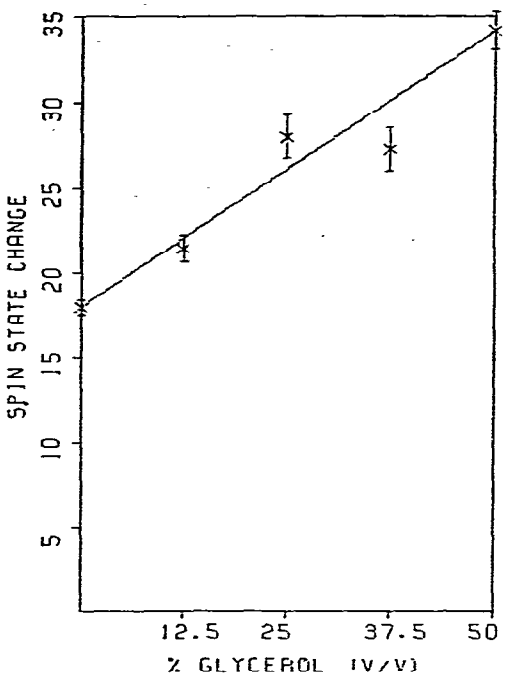


Fig. 7. The variation in ΔSS for $NO_2^-$metHb with (volume) percentage of glycerol as the co-solvent with bis-tris buffer (0.05 M, 0.1 M NaCl, pH 7.0, 5°). [$NO_2^-$] ~ 40 mM, [heme] ~ 100 μM, [IHP] ~ 1 mM (when present).

### 4.2. IHP effect – solvent dependence

The effects of IHP on the spectra of $N_3^-$metHb and $NO_2^-$metHb were measured in four buffer/solvent mixtures, and the result of spin state analysis of these data are given in table 9. Inspection of table 9 reveals that the changes in the spin state distribution with IHP for NO $NO_2^-$metHb are quite sensitive to the solvent composition. The ordering of the magnitudes of ΔSS is phosphate < bis-tris < bis-tris/glycerol ≲ bis-tris/PEG, and the magnitudes more than double through the series of solvents. For $N_3^-$metHb, the IHP-induced changes in the spin state distribution are significantly greater when PEG (MW 190–210) is present. For the other solvents, the trend for $N_3^-$metHb follows that observed for $NO_2^-$metHb, but because the numerical values are within experimental error, a closer comparison is not possible.

We have also measured ΔSS for $NO_2^-$metHb as a function of the percentage of glycerol in the buffer/solvent system. The results are given in fig. 7 and show that the change in spin state with IHP increases monotonically and roughly linearly with the volume percentage of glycerol over the range investigated. Similar results were obtained with PEG as the co-solvent (i.e., rough linearity to 50/50 mixtures).

PEG of high molecular weight has long been used as a means of fractionating protein mixtures by precipitation [45]. On the grounds that solubility and the synergism between IHP and the polyhydroxy solvents might be related, we compared the effect of PEG of different molecular weights. For PEG of molecular weight 6000, precipitation of the protein occurred before enhancement of the IHP effect was observed, unlike the behavior observed for PEG of molecular weight 200. Hence we conclude that the mechanism by which PEG causes protein precipitation, solute exclusion [45], is not the one which enhances the IHP effect.

### 4.3. IHP effect – PEG/glycerol differences

To provide information on any linkage between conformation and ligand binding constant, we measured the apparent binding constant for $NO_2^-$ in the mixed buffer/solvent systems and in the presence and absence of IHP (table 1). Taking the changes in spin state distribution as a measure of conformational change, we see a lack of correlation between conformational change (as ΔSS) and the change in apparent binding constant upon addition of IHP. In the case of bis-tris/glycerol the decrease in binding constant upon addition of IHP correlates with the enhanced spin state changes observed in this solvent. However, in bis-tris/PEG, the spin state changes are the largest observed and yet we see no change in the equilibrium binding constant with IHP. Other differences between the bis-tris/glycerol and bis-tris/PEG cases arise. In the absence of IHP, we see a significant red shift in the HS α band of $F^-$metHb with PEG and none with glycerol. Also PEG and glycerol appear to affect the initial spin state distributions (SS (no IHP), table 9) differently. It therefore appears that PEG and glycerol, even though structurally similar, interact with Hb in different ways.

Table 10

R-form hemoglobins

| Buffer [a] | Hb-Wood SS | Hb-Wood ΔSS | Hb-Osler SS [b] | Hb-Osler ΔSS | DME-treated Hb-A SS | DME-treated Hb-A ΔSS |
|---|---|---|---|---|---|---|
| phosphate/$H_2O$ | 62.7 | 0.9 | – | – [c] | 65.1 | 1.2 |
| bis-tris/$H_2O$ | 61.9 | 3.1 | – | 1.2 | 61.6 | 1.6 |
| bis-tris/glycerol | 63.0 | 1.7 | – | 1.9 | 57.3 | 2.6 |
| bis-tris/PEG | 62.0 | 6.2 | – | 5.0 | 57.7 | 6.2 |

R/T-form hemoglobins

| Buffer [a] | Hb-A SS | Hb-A ΔSS | Hb-S SS [b] | Hb-S ΔSS | Hb-F SS | Hb-F ΔSS |
|---|---|---|---|---|---|---|
| phosphate/$H_2O$ | 66.0 | 13.6 | – [c] | – [c] | 59.2 | 12.5 |
| bis-tris/$H_2O$ | 69.9 | 17.8 | 68.5 | 14.8 | 60.7 | 17.1 |
| bis-tris/glycerol | 70.4 | 26.9 | 70.2 | 30.1 | 59.8 | 34.8 |
| bis-tris/PEG | 63.4 | 30.6 | 64.2 | 27.9 | – [c] | – [c] |

[a] pH 7, diluted 50/50 with the indicated solvent.
[b] This preparation showed ~15% hemichrome, which distorts SS. However, the ΔSS should be ~85% of its correct value.
[c] Missing data.
[d] ΔSS is the difference between SS (with IHP) and SS (no IHP).

### 4.4. IHP effect – mutant or modified hemoglobins

Five additional hemoglobins were chosen to provide a comparison between three with "normal" $O_2$ affinity (Hb-A, Hb-F, and Hb-S) and three with enhanced $O_2$ affinity which can be ascribed to an impediment of the R/T transition. These latter three were Hb-Wood (β97 His → Leu), which lacks one of the $\alpha^1$–$\beta^2$ contacts [46], Hb-Osler (β145 Tyr → Asp), with a modification of the IHP binding site [47], and BME-treated Hb-A with the reagent linking β93 Cys and β97 His [4]. Hb-Wood, Hb-Osler, and BME-Hb all show a reduced cooperativity, enhanced $O_2$ affinity, and reduced response to IHP, relative to Hb-A, in the ferrous form, and so can be said to be stabilized in the R form. These features of the ferrous forms are also reflected in the spin state data for the $NO_2^-$met- forms, given in table 10.

The ΔSS values for Hb-A, Hb-S, and Hb-F are all much higher than those for the R-form set, wherein ΔSS reaches 5% or more only when PEG is present. Clearly the impediments to the R/T transition in the ferrous form carry over to the ferric form and the ΔSS values correlate well with quaternary structure. Since the structural modifications in the R form set vary from modifications of the $\alpha^1$–$\beta^2$ interface to modifications of the COOH terminus of the β chains, we may also conclude from these data that PEG and glycerol are, most probably, influencing the quarternary structure of Hb rather than having any specific pocket or helicity effect.

Another aspect of these data lies in the comparison of the initial spin state distributions (SS) among the several proteins. If the correlation between SS and R/T were a close one, then one would expect the SS values for the R form set to be greater than those for the "normal" hemoglobin. In fact, the SS values for Hb-A and Hb-S are the largest in table 10. (Myoglobin too exhibits a visible MCD spectrum which appears to have a much larger HS contribution than Hb-A does, even though Mb is a common model for an R form hemoglobin.)

### 4.5. IHP effect – estimation of the R/T populations

Since it is clear that ΔSS provides a measure of the conversion of R form metHb to T form metHb, it is incumbent on us to explore the possibility that ΔSS can be used to evaluate the allosteric constant in $NO_2^-$metHb, $L$ (≡[T]/[R]). Such a calculation requires two reference points, namely the SS-values for pure R and pure T forms. It is clear from the data presented in the previous section that such points are not applicable to all hemoglobins. However, if one refers only to one protein, say Hb-A, and assumes values (or at least limits) for the SS values of R and T forms, then one can estimate $L$ under intermediate conditions. If we assume that $NO_2^-$metHb-A is ~70% low spin in the R form (bis-tris, no IHP, table 9) and ~33% low spin in the T form (bis-tris/PEG, with IHP, table 9), calculations indicate that the proportions of the R and T forms, *in the presence of IHP*, in phosphate or bis-tris buffers are about equal.

## 5. Conclusions

We have found that PEG (MW 190–210) and glycerol enhance the spectral changes induced by IHP in $NO_2^-$metHb. We interpret these enhanced spectral changes as an indication that IHP induces more complete

R/T transition in these solvents, as opposed to a lesser effect in aqueous buffers. Calculations based on the two state model, assuming the above-stated SS-values for the pure R and T forms, indicate that the populations of R and T states are roughly equal for $NO_2^-$metHb. *in the presence of IHP*, and in phosphate or bis-tris buffer.

These conclusions make the data presented by Perutz and co-workers [6,7] on trout Hb much more understandable. Hb-A is apparently only partially converted to the T form by IHP in the usual buffers whereas trout Hb seems to be completely so converted. The added effect of glycerol or PEG makes Hb-A approach trout Hb in its ability to undergo the R/T transition.

Certain differences between glycerol and PEG do appear. PEG shifts the spectra of $F^-$metHb-A, which is presumably biased towards the T form by virtue of being high spin, in the same way that IHP does. PEG also makes all of the R form hemoglobins and $N_3^-$metHb-A exhibit their largest spin state changes with IHP. Glycerol does neither. Also, there is a factor of two difference between the apparent binding constants of $NO_2^-$ to $H_2O$metHb in these two buffer/solvent mixtures.

Finally, a comparison of several hemoglobins shows that while the *changes* in spin state distribution with IHP (ΔSS) correlate with changes in quarternary structure for a particular hemoglobin, there is no similar correlation between quarternary structure and the initial SS values among the various hemoglobins examined here.

## References


[1] M.F. Perutz, Nature 228 (1970) 726.
[2] M.F. Perutz, Nature 237 (1972) 495.
[3] M.F. Perutz, J.E. Ladner, S.R. Simon and C. Ho, Biochem. 13 (1974) 2163.
[4] M.F. Perutz, A.R. Fersht, S.R. Simon and G.C.K. Roberts, Biochem. 13 (1974) 2174.
[5] M.F. Perutz, E.J. Heidner, J.E. Ladner, J.G. Beetlestone, C. Ho, and E.F. Slade, Biochem. 13 (1974) 2187.
[6] M.F. Perutz, J.K.M. Sanders, D.H. Chenery, R.W. Noble, R.R. Pennelly, L.W.M. Fung, C. Ho, I. Giannini, D. Pörschke, and H. Winkler, Biochem. 17 (1978) 3640.
[7] C. Messana, M. Cerdonio, P. Shenkin, R.W. Noble, G. Fermi, R.N. Perutz and M.F. Perutz, Biochem. 17 (1978) 3652.
[8] R.C. Ladner, E.J. Heidner and M.F. Perutz, J. Mol. Biol. 114 (1977) 385.
[9] V.E. Shashoua, in: Hemes and hemeproteins, eds. B. Chance, R.W. Estabrook and T. Yonetani, (Academic Press, N.Y., 1966).
[10] M.V. Volkenstein, Y.A. Sharonov, and A.K. Shemelin, Nature 209 (1966) 709.
[11] C. Djerassi, E. Bunnenberg and D.L. Eider Pure and Appl. Chem. 25 (1971) 57.
[12] N.A. Sharonova, Y.A. Sharonov, and M.V. Volkenstein, Biochim. Biophys. Acta 271 (1972) 65.
[13] Y.A. Sharonov and N.A. Sharonova, FEBS Letters 27 (1972) 221.
[14] H. Rein, K. Ruckpaul and W. Haberditzl, Chem. Phys. Lett. 20 (1973) 71.
[15] H. Rein, K. Ruckpaul and W. Haberditzl, FEBS Letters 37 (1973) 166.
[16] H. Rein, O. Pistau and K. Ruckpaul, Biochim. Biophys. Acta 393 (1975) 373.
[17] S. Yoshida, T. Iizuka, T. Nozawa and M. Hatano, Biochim. Biophys. Acta 405 (1975) 122.
[18] J.I. Treu and J.J. Hopfield, J. Chem. Phys. 63 (1975) 613.
[19] H. Kobayashi, Adv. Biophys. 8 (1975) 191.
[20] Y.A. Sharonov, N.A. Sharonova and B.P. Atanosov, Biochim. Biophys. Acta 434 (1976) 440.
[21] Y.A. Sharonov and N.A. Sharonova, Biochim. Biophys. Acta 446 (1976) 547.
[22] P.J. Stephens, J.C. Sutherland and J.C. Cheng, in: Excited states of biological molecules, ed. J.B. Birks, (Wiley, N.Y., 1976) p. 434.
[23] M.A. Livshitz, A.M. Arutyunyan, and Y.A. Sharonov, J. Chem. Phys. 64 (1976) 1276.
[24] M. Kajiyoshi and F.K. Anan, J. Biochem. 81 (1977) 1327.
[25] Y.A. Sharonov, A.P. Minezev, M.A. Livshitz, N.A. Sharonova, V.B. Zhurkin and Y.P. Lysov, Biophys. Struct. Mechanism 4 (1978) 139.
[26] W.A. Eaton, L.K. Hanson, P.J. Stephens, J.C. Sutherland, and J.B.R. Dunn, J. Am. Chem. Soc. 100 (1978) 4991.
[27] L. Vickery, T. Nozawa and K. Sauer, J. Am. Chem. Soc. 98 (1976) 343.
[28] J.H. Dawson, J.R. Trudell, R.E. Linder, G. Barth, E. Bunnenberg, and C. Djerassi, Biochem. 17 (1978) 33.
[29] J.L. Hoard, in: Hemes and Hemeproteins, eds. B. Chance, R.W. Estabrook and T. Yonetani (Academic Press, New York, 1966) p. 9.
[30] J.L. Hoard, Science 174 (1971) 1295.
[31] R.E. Linder, R. Records, G. Barth, E. Bunnenberg, C. Djerassi, B.E. Hedlund, A. Rosenberg, E.S. Benson, L. Seamans, and A. Moscowitz, Anal. Biochem. 90 (1978) 474.
[32] A.D. Barksdale, B.E. Hedlund, B.E. Hallaway, E.S. Benson and A. Rosenberg, Biochem. 14 (1975) 2695.
[33] J. Bello and H.R. Bello, Arch. Biochem. Biophys. 172 (1976) 608.
[34] P.R. Bevington, Data reduction and error analysis for the physical sciences, Ch. 9 (McGraw-Hill, NY, 1969).
[35] P.J. Stephens, J. Chem. Phys. 52 (1970) 3489.
[36] P.J. Stephens, Adv. Chem. Phys. 35 (1976) 197.

[37] P.J. Stephens, R.L. Mowery and P.N. Schatz, J. Chem. Phys. 55 (1971) 224.
[38] R.D.B. Fraser and E. Suzuki, in Spectral Analysis: Methods and Techniques, ed. J.A. Blackburn (Marcel Dekker, NY, 1970) p. 171.
[39] M.E. Magar, Data analysis in biochemistry and biophysics (Academic Press, NY, 1972) p. 143.
[40] M.D. McKay, private communication.
[41] D.W. Smith and R.J.P. Williams, Biochem. J. 110 (1968) 297; Structure and Bonding 7 (1970) 1.
[42] T. Iizuka and M. Kotani, Biochim. Biophys. Acta 194 (1969) 351.
[43] T. Iizuka and T. Yonetani, Adv. Biophys. 1 (1970) 157.
[44] W.A. Eaton and R.M. Hochstrasser, J. Chem. Phys. 49 (1968) 985.
[45] K.C. Ingham. Arch. Biochim. Bipohys. 186 (1978) 106.
[46] F. Taketa, Y.P. Huang, J.A. Libuoch and B.H. Dessel, Biochim. Biophys. Acta 400 (1975) 348.
[47] A. Arnone, G. Gacon and H. Wajeman, J. Biol. Chem. 251 (1976) 5875.